Experimental Investigation on Single-Medium Stratified Thermal Energy Storage System

S. Advaith [a], Dipti Ranjan Parida [b], K. T. Aswathi [b], Nikhil Dani [b], Utpal Kumar Chetia [b], Kamanio Chattopadhyay [c], Saptarshi Basu [a, b,*]

[a] Interdisciplinary Centre for Energy Research (ICER), Indian Institute of Science, Bangalore 560012, India
[b] Department of Mechanical Engineering, Indian Institute of Science, Bangalore 560012, India
[c] Department of Materials Engineering, Indian Institute of Science, Bangalore 560012, India
* Corresponding Author email: sbasu@iisc.ac.in

Abstract

The demand for renewable energy sources is limited by their inherent intermittent nature. The thermal energy storage technique overcomes this shortcoming by allowing storage of naturally occurring energy (e.g. solar) during "non-peak hours". The article presents an experimental investigation of the sparsely studied 'single medium thermocline' (SMT) based single tank sensible thermal energy storage (TES). The work aims to reconsider its potential by minimizing the fluid dynamic perturbations during the charging cycle which disrupt the stability of the thermocline leading to undesirable energy losses. The article discusses the effect of Atwood number (density stratification) and mean temperature on TES effectiveness as well as providing the appropriate thermodynamic insights. Implementation of the experimental procedures and strategies discussed in this article demonstrates a stable thermocline which persists for more than six hours with minimal energy degradation.

Keywords: Thermal energy storage, Thermocline, Single medium, Single tank, Thermal stratification

Nomenclature

A_t	Atwood number $(\rho_c - \rho_h)/(\rho_c + \rho_h)$,-
C_p	Specific heat, kJ/kg K
E_t	Total thermal energy at time 't', J
E_1	Total thermal energy at time 't = 60 minutes', J
E*	Normalized energy (E_t / E_1), -
H	Height of the tank, m
h*	Non-dimensional axial distance (y/H), -
k	Thermal conductivity, W/m K
m	Mass, Kg
T	Instantaneous temperature, K
t	Time, s
t_1	Time 't = 60 minutes', s
T_c	Cold fluid temperature, K
T_h	Hot fluid temperature, K
T_m	Mean temperature inside the thermocline region, K
T_0	Ambient temperature, K
T*	Non-dimensional temperature $((T-T_c)/(T_h-T_c))$, -

ΔT	Initial temperature difference (T_h-T_c), K
V_i	Volume of i^{th} fluid section, m^3
y	Axial (vertical) direction, m

Greek symbols

ρ	Density, kg/m^3
ρ_i	Density of i^{th} fluid section
ρ_c	Fluid density at cold fluid temperature, kg/m^3
ρ_h	Fluid density at hot fluid temperature, kg/m^3
τ	Normalized storage time (t/t_1), -
ξ_m	Exergy of the fully mixed storage, J
ξ_t	Exergy of the stratified storage at any time t, J
$\xi^{\#}$	Rosen's exergy ratio (ξ_e/ξ_m), -
ξ^*	Normalized exergy (ξ_t/ξ_1), -

Abbreviations

CSP	Concentrated Solar Power
DMT	Dual medium thermocline
HSM	Heat storage media
IEA	International Energy Agency
PV	Photovoltaics
STES	Sensible thermal energy systems
STE	Solar thermal energy
SMT	Single medium thermocline
SSTES	Stratified sensible TES
TES	Thermal energy storage

1. Introduction

The demand for energy has reached unprecedented levels with the ever-rising industrialization and global population surge. This has initiated a global initiative towards clean, affordable, sustainable, and reliable sources of energy. The fact that energy could solve most of the challenges and create ample opportunities in today's world is indisputable. According to the United Nations, assurance of universal access to such energy resources to everyone is indispensable [1]. Among the renewable energy sources, sun is undoubtedly the most promising one, considering its limitless potential and versatility. However, there is a chance for mismatch between the supply and demand because of its intermittent nature (clouds and night hours), which in turn compel us to incorporate solar energy storage. Such storage systems are essential in various fields, including power generation sectors like solar thermal, geothermal, and nuclear power plants.

Thermal energy storage systems, in contrast to battery storage in (photovoltaic) PV systems, depend on renewable thermal energy sources [2]. STE systems are relatively inexpensive for large scale and robust operations as compared to alternative technologies. It enhances the effectiveness and efficiency of the Concentrated Solar Power (CSP) applications by aiding the generation of power even after sunset or during cloud cover [3], [4]. The recent progress in materials has revolutionized thermal energy storage (TES) technologies [5].

The thermal energy is generally stored either through modification of temperature of a material (sensible heat) or by phase change of a substance (latent heat). Sometimes, both of these methods are combined to come up with a hybrid TES technology capable of serving a more extensive operating range. However, sensible thermal energy systems (STES) are relatively inexpensive and straightforward with regards to operation and maintenance which makes them one of the most popular and commercially viable thermal energy storage method. STES utilizes heat transfer fluids which are stable at high temperatures. The method depends not only on the mass, specific heat capacity, and change in temperature of the storage medium [6] but also on additional factors like diffusivity, thermal conductivity, stability, material compatibility, and the cost. Among the sensible thermal energy storage methods, stratified sensible TES (SSTES) system has been investigated for more than four decades [7]-[9] since it lowers the cost of power generation by significantly cutting down the total setup cost [10]. Additionally, the inherent simplicity of this technology enables efficient scaling to meet a wide range of power requirements [11]. Thus, it overcomes the limitations of existing technologies and can play an instrumental role in transforming the solar energy landscape. For these reasons, it is preferred over the other variants (like two tank method) and is investigated in the current study.

The principle of SSTES is inspired by the natural thermal stratification process where, the hot and cold fluids are stored in an inherently stable stratified configuration. They are separated by a narrow region of a large density gradient called 'thermocline' as shown in Figure 1c. The thermocline facilitates the storage of energy in the media [12]. Its stability is one of the crucial factors that govern the energy efficiency of a single tank TES and the associated system [13], [14]. The operation of a TES with density stratification involves sequential charging and discharging cycles (Figure 1). During charging, hot fluid coming from the solar collection field enters into the top of the tank as cold fluid exits from the bottom to be heated as shown in Figure 1 a. During discharging, hot fluid from the top is pumped to the power block to generate electricity and returns to the tank at a relatively colder temperature as shown in Figure 1 b.

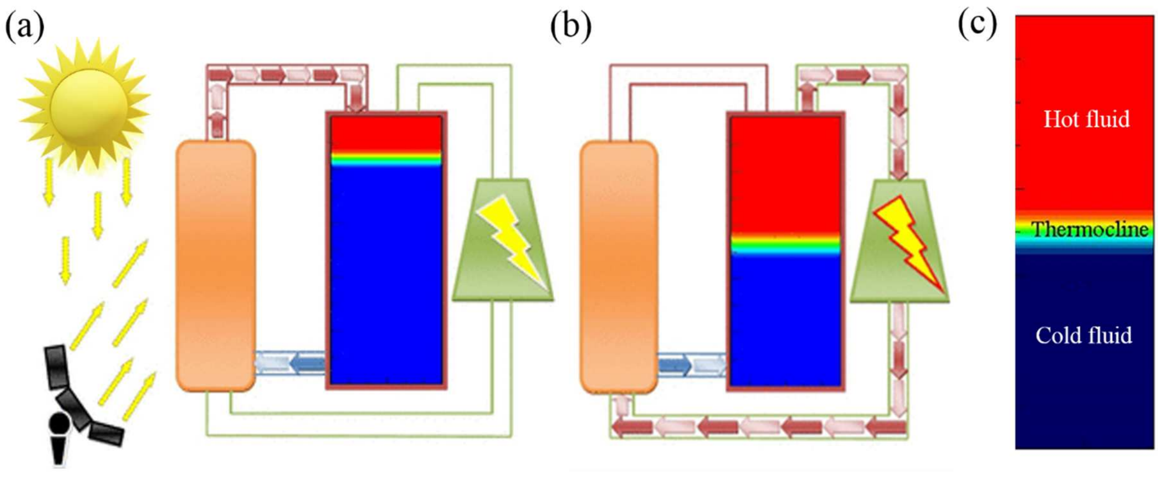

Figure 1: (Colour): Density stratified thermal energy storage operations (a) Charging process (b) Discharging process (c) Schematic of density stratified single tank thermal energy storage

In a single tank system, two thermocline techniques are commonly adopted, viz., (Single medium thermocline) SMT and (Dual medium thermocline) DMT. DMT is typically composed of a fluid HSM (Heat storage media) and solid filler materials while SMT is composed HSM only. Patcheco et al. [15] found that cost reduction can be attained upon using appropriate filler materials in a DMT. As a result, there has been a surge in the studies on DMT. This led to a shift of focus from studies on SMT which also involve internal fluid flow and their associated mixing issues. The number of experimental and numerical studies pertaining to packed-bed thermal energy storage is constantly increasing over the past years [16]-[18].

However, DMT also presents technical difficulties such as thermal ratcheting [19], maintenance issues due to unwanted particle deposition and the hassle of appropriate pairing of filler material and storage media [20]. There is also a possibility of having unstable storage capacities for a DMT based systems because of the increase in outlet temperature of heat transfer medium during charging. However, this issue doesn't arise in case of SMT since a constant outlet temperature is maintained throughout [21]. In addition, greater thermal diffusion is observed in the DMT tank, which elongates the heat-exchange region along with the height of the porous region [22]. Furthermore, the trouble of thermocline thickening, and oil degradation occur as a consequence of choosing an inappropriate or incompatible filler material. Thus, prior works are required since the filler material cannot be chosen randomly. SMT avoids all the above-mentioned complications, although its fluid dynamic problems and cost issues still pose a substantial challenge. Furthermore, unlike DMT, an internal heat exchange between the heat transfer fluid and the storage medium is not necessary in SMT which avoids associated heat losses. Under adiabatic conditions of operation, both the units have high thermal performance, with slightly higher first and second law efficiencies for SMT as compared to DMT [22], [23]. Effective mitigation of fluid dynamical perturbations and the cost advantage of DMT with filler materials could have been the reasons behind lesser number of studies in SMT. Based on the aforementioned discussion, an extensive study on SMTs is attempted here. However, to the best of authors’ knowledge, there is no experimental analysis of SMT available in literature other than the one presented by Gajbhiye et.al. [24] where the thermocline formation is analyzed for three different mass flow rates for a fixed stratification strength with water as the HSM. We conducted a few prior studies in order to mitigate the fluid dynamical perturbation inside an SMT tank. It has been found that the resistance towards mixing in a density stratified layer can be assessed from the relative strength of stratification and that of the impinging fluid [25]. Thus, it is also important to analyze the SMT system by varying the strength of stratification for a fixed flow rate.

The present study is intended to explore the challenges associated with the fluid flow problems associated with SMT system. Care has been taken to conduct the experimental studies under near adiabatic conditions. For the study, we have chosen Hytherm-600 (a synthetic oil) as HSM because of its wider operating range (unlike water) and absence of solidification issues or corrosive problems like molten salt. Moreover, it is suitable for medium-scale applications especially pertaining to small-scale industries. In the present study, a lab-scale experimental facility is developed to demonstrate the efficacy of a SMT based single-tank sensible energy storage system. The results are quite useful for the design and validation of thermocline storage systems, considering the scarcity of experimental investigations in the literature. Moreover, a series of empirical studies are performed by varying mean temperature and stratification strength to compare TES effectiveness.

2. Experimental facility and methodology

A single tank single medium stratified thermal energy storage system is designed and developed at the Interdisciplinary Centre for Energy Research (ICER), IISc Bangalore. The experimental setup is schematically shown in Figure 2**.** The solar energy is simulated with the help of a two-stage heating system with a net power rating of 35kW. The first stage of heating is carried out in an inventory tank. Subsequently, the energy storage medium is pumped via a customized vertical centrifugal pump to a heat receiver where the second level of heating is carried out. The entire facility is designed to withstand high temperatures and is made up of high-temperature corrosion-resistant material, Inconel 600. Detailed specifications of all the major components are provided in Appendix A (Table 2).

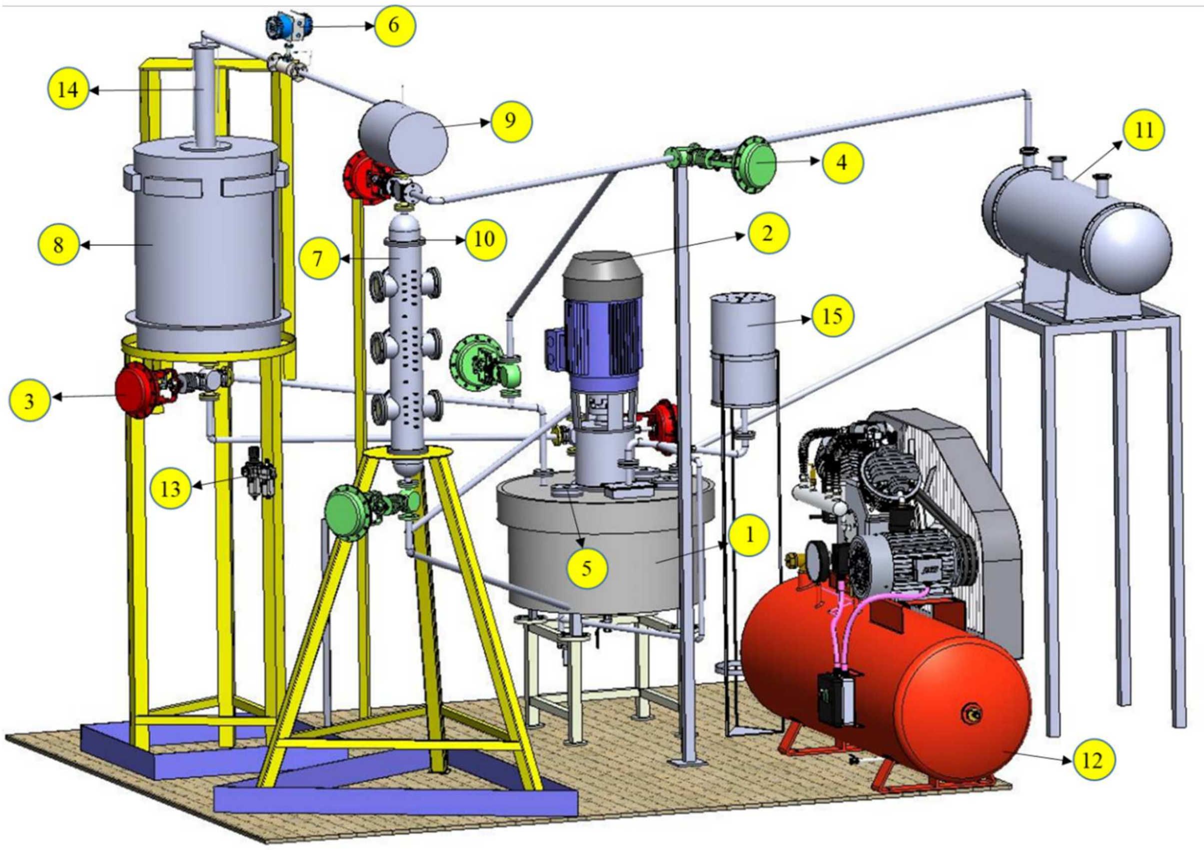

Figure 2 (Colour): Experimental schematic, 1-Inventory tank, 2-VFD controlled centrifugal pump, 3-Three-way directional valves, 4-Normally closed two-way directional valve, 5-Immersion heaters, 6-Flow meter, 7-Thermal energy storage tank, 8-Heat receiver with split type heater, 9-Filler tank, 10-Distributor, 11-Heat exchanger, 12- Compressor, 13- Air regulator and filter, 14- Ceramic wool insulation with aluminium cladding, 15-Surge tank

Operational procedure

The heat transfer-cum-storage fluid is introduced into the inventory tank via an inlet at the top and is heated to a temperature 'T_c' (referred as cold fluid temperature) (Figure 3). Circulation of HSM, while immersion heaters are in operation, is essential to avoid localised boiling near the heater surface. As soon as the temperature measured by a K-type (Chromel - Alumel) thermocouples on the inventory tank attain 'T_c', the HSM is routed to the TES tank using a vertical axis centrifugal pump and an associated Variable Frequency Drive (VFD). A coriolis multipurpose flow meter is used to maintain appropriate flow rate. After the TES is filled up at temperature T_c, the 25kW heaters associated with the heat receiver as well as the immersion heaters are activated to heat the HSM to a higher temperature $T_h > Tc,$ which is then allowed to fill the storage tank through a distributor for smooth streamlined flow. This ensures that minimal mixing happens within the TES to establish a stable and thin thermocline. While HSM at temperature T_h fills the TES through the top, cold HSM is simultaneously drawn out from the bottom. The displaced fluid is collected back to the inventory tank. This process of storing energy within the TES is referred to as the 'charging phase'. Thermocouple array installed on TES records real-time axial temperature distribution, which is monitored via a graphical user interface (GUI) and recorded for a desirable duration at high acquisition rate using NI LabVIEW assisted software.

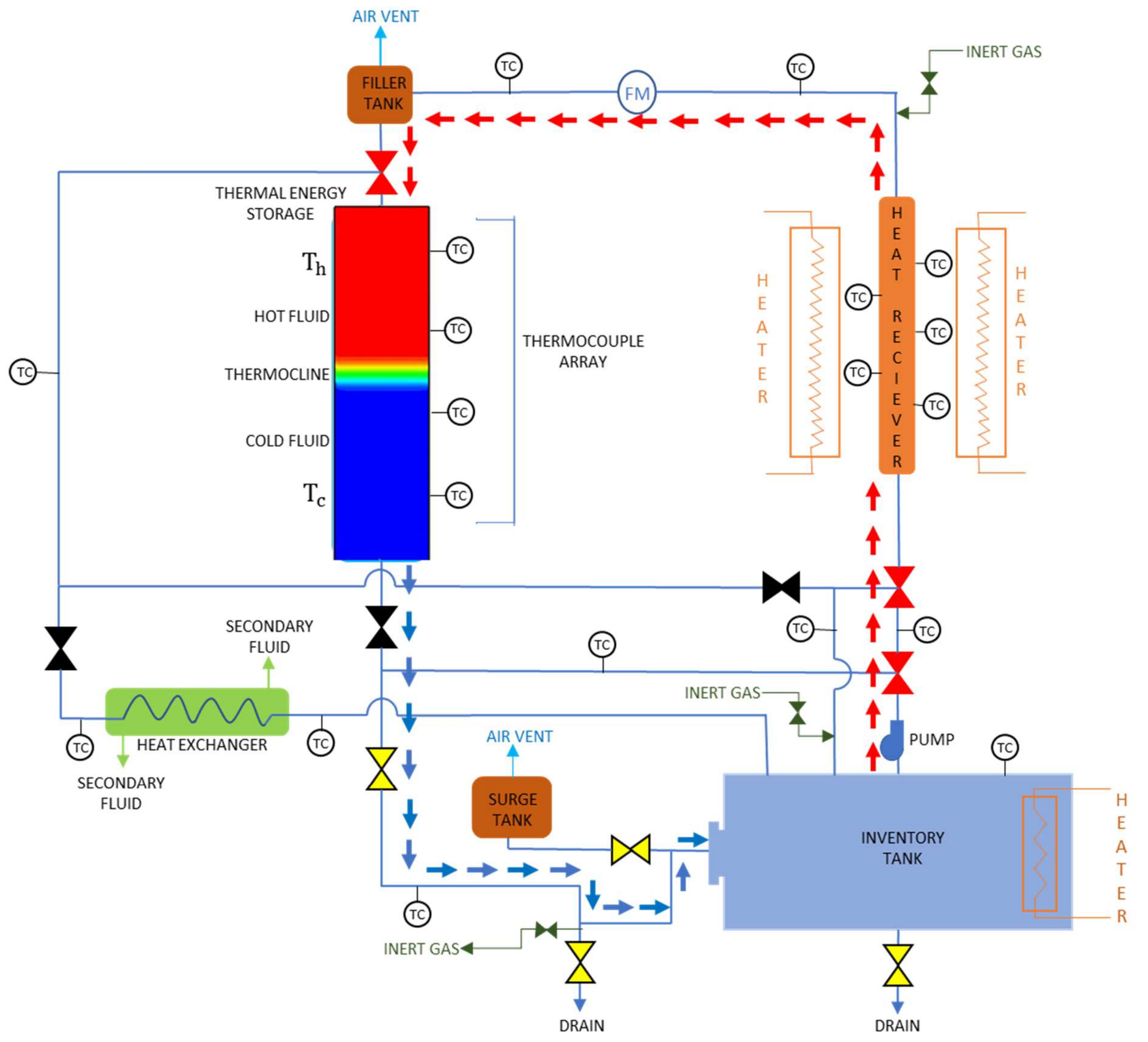

Figure 3 Colour): Charging operation of the sensible thermocline thermal energy storage

Energy is thus stored in the form of sensible heat in the storage material. This phase is referred to as the 'storing phase' which the current study focuses upon. The following preventive measures are taken to minimize heat losses. The TES is covered with a thick (50 mm) ceramic wool insulation (K=0.12 $Wm^{-1}k^{-1}$) and cladded with aluminium sheets to curtail convective heat loss. Besides, the ceramic coating inside the TES wall diminishes axial wall conduction. The inlet distributor restrains mixing during the charging of TES. These strategies facilitated in maintaining a stable and sustainable thermocline even after 6 hours. Finally, during 'discharging process', the HSM is cooled down through a shell and tube heat exchanger and is eventually drained out.

Focus of the study

The primary focus of the study is to develop an effective single medium thermocline based thermal energy storage with minimal mixing leading to better stability of the thermocline during the storing phase. The resistance against mixing of the thermal stratification is quantified in terms of the Atwood number ($A_t = (\rho_c - \rho_h)/(\rho_c + \rho_h)$) where, ρ_c, ρ_h are densities of cold and hot fluids respectively. Different scenarios are considered by varying the Atwood number from 0.01 to 0.03 while maintaining nearly constant mass flow rate for all cases (Re ≈1500). This is done while keeping the cold fluid at the ambient condition.

Subsequently, non-ambient cold fluid scenarios are compared with ambient condition to see whether there is any significant drop in storage effectiveness while maintaining same $\Delta T = T_h - T_c$. This is done to extend the scope of the current work to high temperatures while taking into account the molten-salt characteristics (i.e., a non-ambient operating T_c) owing to its high melting point. Although in many practical applications, molten salts are widely used due to their high- temperature operational range, the current work is restricted to Hytherm-600 oil. The thermophysical properties of the storage media (Hytherm-600 oil) within the operating range of 298 to 573K are calculated based on the following empirical relations

$$\rho\,(T) = 1049.7 - 0.6572T \;\; Kg/m^3 \tag{1}$$

$$C_P(T) = 0.00002T^2 - 0.0096T + 2.3169\, JKg^{-1}K^{-1} \tag{2}$$

$$K\,(T) = -0.0346 + 0.0007T\; Wm^{-1}K^{-1} \tag{3}$$

The cases considered are depicted in the Table 1. It is to be noted that since the boiling point of Hytherm 600 is higher than water, unwanted effects like vapor formation are avoided in the chosen operating range.

Table 1: Experimental cases

Case	T_c (^{0}C)	T_h (^{0}C)	ΔT(^{0}C)	T_C/T_0	A_t
A	25	50	25	1	0.01
B	25	75	50	1	0.02
C	25	100	75	1	0.03
D	45	95	50	1.8	0.02
E	60	110	50	2.4	0.02

3. Results and discussion

Two different scenarios are considered here; one with ambient cold fluid temperature ($T_c = T_0$) and the other with non-ambient temperature T_c. Transient analysis is avoided to focus more on the thermal degradation of the thermocline. Here, the storage time (t) is non-dimensionalized as $\tau = t/60$ minutes,. The observed temporal characteristic of the axial temperature profiles fit well with the sigmoid function previously reported [26].

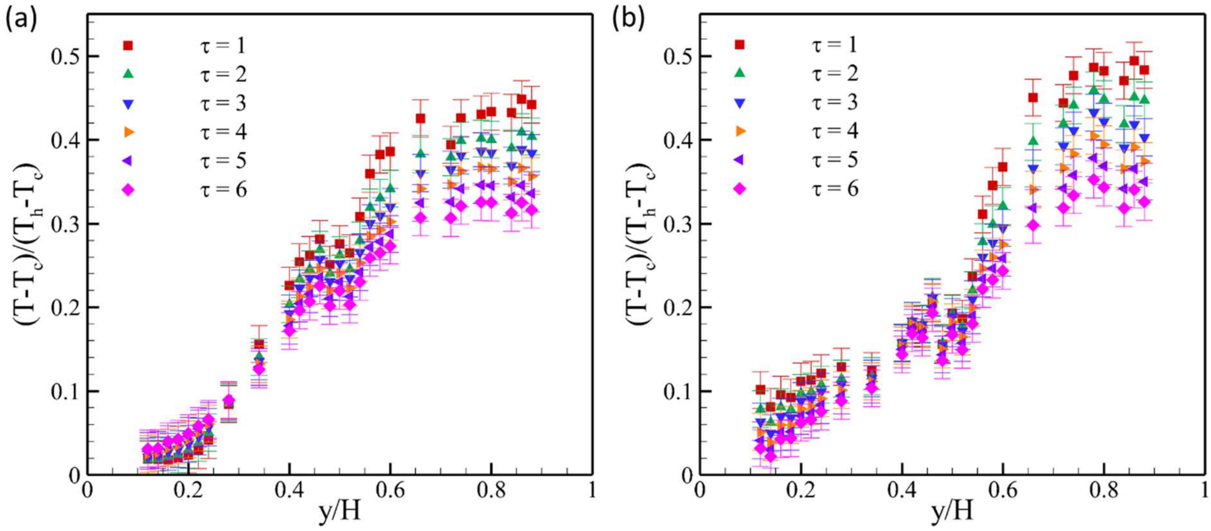

Figure 4 (Colour): The normalised temperature $T^* = ((T - T_c)/(T_h - T_c))$ *plotted against normalised tank height* $h^* = (y/H)$ *for six hours with one-hour gap. (a): Non dimensionalized temperature profile,* $T_C/T_0 = 1$ *,* A_t *= 0.02,* $\Delta T = 50^0 C$ *(b): Non dimensionalized temperature profile,* $T_C/T_0 = 1.8$ *,* $A_t \approx$ *0.02,* $\Delta T = 50^0 C$

Figure 4 (a) shows that the colder fluid gained thermal energy over time while the hotter fluid temperature dropped significantly. Heat exchange with the environment, axial wall conduction through the tank wall, and thermal diffusion within the tank cause degradation of energy in the hotter fluid as reflected through its temperature drop. A fraction of the losses via thermal diffusion and axial wall conduction results in consequent thermal energy gain of the colder fluid.

Figure 4 (b) suggests that stable and sustainable thermocline is formed even at non-ambient cold fluid condition. In contrast to the earlier case, both colder as well as hotter fluid temperatures, decays over time, with the latter at a faster rate due to its higher heat exchange potential with the environment. It can be observed that the heat gained by the cold fluid over time in the non-ambient case is lower than that in the ambient case. This is due to the fact that the rate of heat loss in cold fluid is higher than the rate of heat gain from the hot fluid.

Further, there could be variations in the profile achieved upon varying stratification strength and the corresponding mean temperature. This will be studied in the subsequent subsections.

3.1. Effect of Atwood number

The axial variation in the temperature of the HSM is plotted for three different Atwood numbers for two distinct storage time instances in Figure *5*. Atwood number is varied here by changing only the hot fluid temperature while maintaining the cold fluid temperature the same as that of the ambient.

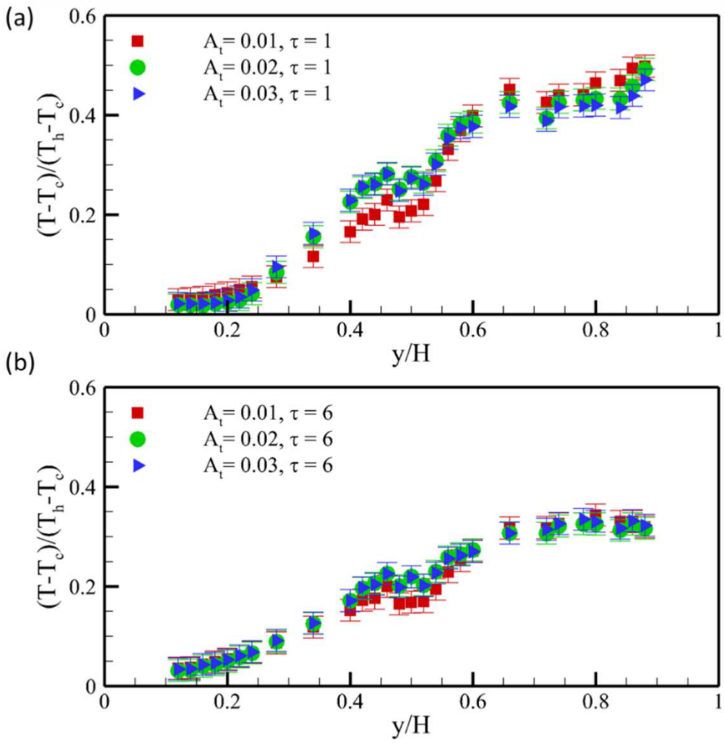

Figure 5 (Colour): The normalised temperature $T^* = ((T - T_c)/(T_h - T_c))$ plotted against tank height $h^* = (y/H)$ for cases with ambient cold fluid condition, $T_C/T_0 = 1$ but distinct Atwood numbers for two distinct storage time instants (a) 60min (b) 360min

It is observed that the curves corresponding to distinct Atwood numbers collapse into a single one, except at around y/H = 0.5 (thermocline region) irrespective of the storage time instant. In other words, in the case of the ambient cold fluid condition at a specific storage time instant, the normalized temperature profile is independent of the stratification strength (A_t) except at the thermocline region. An increase in Atwood number indicates a rise in the density difference, which in turn favors the stability of the thermocline. It appears that same initial trend in the profile is sustained even after 5 hours of operation. The dependence on initial ΔT is evident here and shows the importance of charging process in the formation of a stable and sustainable thermocline. A dip in temperature observed for A_t=0.01 is because of the increased mixing across the thermocline induced during the charging process. However, in the case of A_t= 0.02 and 0.03, the thermocline strength is sufficient to cause a decay in the initial disturbance. Although this provides insights towards developing an analogous regime map to predict the resistance of thermal stratification towards mixing during charging, it is beyond the scope of the current study.

3.2. Effect of the mean temperature

The axial variation in the temperature of the heat storage media is plotted for distinct cold fluid temperature scenarios while maintaining the same temperature difference ($\Delta T = T_h - T_c$) between the corresponding hot fluid at the time of charging. The initial temperatures of both the fluids (T_h and T_c) are higher resulting in a higher mean temperature (T_m). Three such cases (B, D and E) are compared in Figure *6* for two distinct storage time instances. We maintain constant ΔT, to ensure nearly same A_t (owing to the linear density dependence of HSM under consideration).

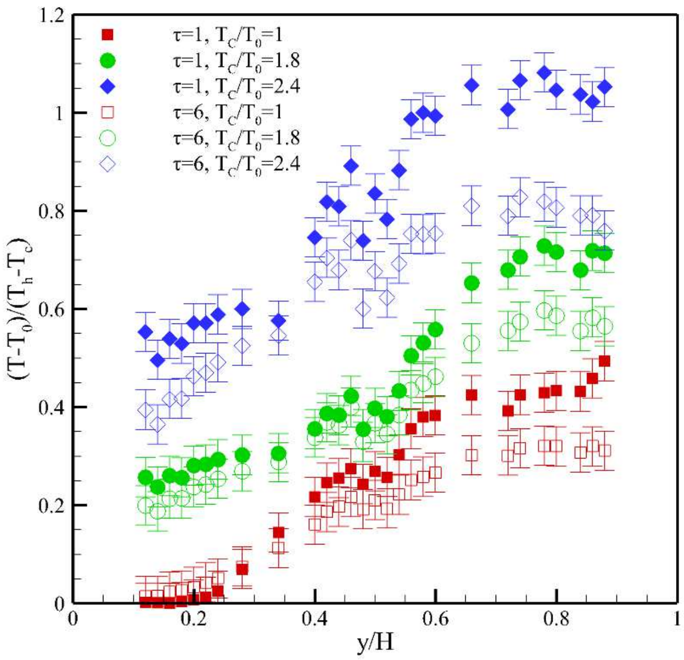

Figure 6 (Colour): The normalised temperature $T\# = ((T - T_0)/(T_h - T_c))$ *plotted against normalised tank height for cases having same* $\Delta T = (T_h - T_c) = 50^0C$ $(A_t \approx 0.02)$ *but distinct cold fluid temperature* T_c *for storage time instants* $\tau = 1$ *and* 6.

The area under the curve is an indication of the amount of stored thermal energy. It can be observed that, higher the mean temperature, higher is the energy content. Also, the trend is maintained during all storage time instances. The mean temperature (in K) of Case B ($T_c/T_0 = 1$) after 5 hours is observed to be 0.97% lesser than the initial measurement. However, this decrease is 1.05% and 2.5% for Case D ($T_c/T_0 = 1.8$) and Case E ($T_c/T_0 = 2$) respectively. Unlike the non-ambient cases, cold fluid temperature is enhanced as explained in Figure 4 b and this is reflected in the mean temperature as well.

By taking any two τ = 1 and 6 pairs, it can be seen that the temperatures and thus the energy contents degrade at different rates. Since the temperature at each axial location degrades at different rates, T_m provides us with only an approximate way of comparing overall energy. In terms of sustainability, it is imperative to analyse the rate of energy degradation. Such rates as well as the magnitude of energy and its effectiveness can be better understood by conducting a thermodynamic analysis as shown in the following section.

3.3. Thermodynamic analysis

The stratified thermal energy storage with uniform cross-section is partitioned into 'n' horizontal layers in such a way that each fluid section 'i' with volume (V_i) contains a thermocouple representing the bulk temperature of that section (T_i), for this analysis. Due to stratification, the thermophysical properties of the storage media change with temperature. The variation in density (ρ_i), heat capacity (C_{P_i}), and conductivity (K_i) for each section 'i' are considered here as per equations (1-3).

Assumptions:

(a) TES is a closed system during the storage phase (there is no exchange of storage media during the storage phase)
(b) The kinetic and potential energies are neglected here (i.e., total energy = internal energy)
(c) Circumferential and radial variations of temperature are neglected in comparison with its axial variation

The first law of thermodynamics applied to the section ‘i’ for time ‘t’ can be written as

$$\rho_i V_i \Delta u_{i,t} = E_{i,t} - W_{i,t} \quad (4)$$

Where $\Delta u_{i,t}$, $E_{i,t}$, $W_{i,t}$ are specific internal energy change, net thermal energy and net work done by the system on its surroundings respectively in i^{th} section at time t.

The total thermal energy in the TES at any time ‘t’ can be written as,

$$E_t = \sum_{i=1}^{n} \rho_i V_i (C_P)_i [T_{i.t} - T_0] \quad (5)$$

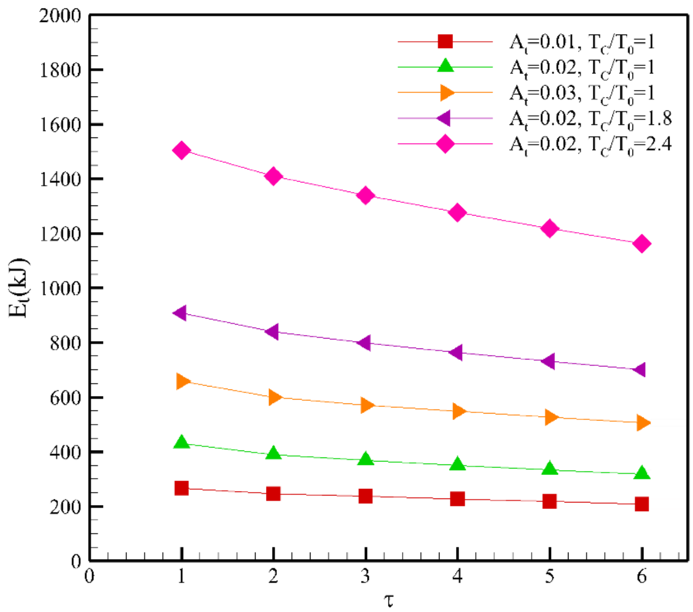

Figure 7 (Colour): The total thermal energy in the TES at any time ‘t’, E_t plotted against the normalized time, $\tau = t/t_1$ (t_1 = 60 minutes) illustrates the relative decay rate of energy

Figure 7, shows that by increasing both Atwood number and mean temperature, one could store more quantity of energy, although with a higher rate of degradation. However, evaluating the TES performance based on energy efficiencies could be misleading since it considers only the ratio of the heat recovered to the heat input while ignoring the concomitant temperature and thus the quality of energy. Figure 7 shows the total energy of the system at different time instances and consequently estimates the total energy lost from the system. In order to quantify the useful work which can be extracted from a system, after addressing the irreversibility induced through internal mixing, an exergy analysis is presented here. Exergy based evaluations provide a better estimate of TES usefulness as it considers both energy quality as well as quantity.

The second law of thermodynamics applied to section ‘i’ for time ‘t’ can be written as

$$\rho_i V_i \Delta s_{i,t} \geq \int_t^{t_0} \frac{dE_{i,t}}{T_i} \tag{6}$$

Where $\Delta s_{i,t}$– change in specific entropy on i[th] section at time t, t_0 – time taken to reach ‘dead state’ (a state where the tank is fully discharged)

The entropy in a closed system is not constant unlike energy. The entropy changes of a TES system (ΔS_s) may be caused by

(a) The net mass transfer across the system boundaries as indicated by ΔS_f
(b) The heat transfer across system boundary (ΔS_h)
(c) Internal entropy generation (S_g)

The internal entropy generation of the process (S_g) is,

$$S_g = \Delta S_s - \Delta S_f - \Delta S_h \geq 0 \tag{7}$$

During the energy storage phase of TES, ΔS_f and ΔS_h are generally neglected.

$$\rho_i V_i \Delta s_{i,t} = \int_t^{t_0} \frac{dE_{i,t}}{T_i} + S_g \tag{8}$$

Since the enthalpy content of the TES does not gets altered due to internal mixing, the internal exergy loss (ξ_d) of a TES is directly proportional to the internal entropy generation.

$$\xi_d = -T_0 S_g \tag{9}$$

Where, T_0 is the thermodynamic dead-state temperature.

The change in exergy of i[th] section from time ‘t’ to a state where the tank is totally discharged results in

$$\xi_{i,t} = \rho_i V_i C_{P_i} (T_{i.t} - T_0) - T_0\, \rho_i V_i C_{P_i} \ln\left(\frac{T_{i,t}}{T_0}\right) \tag{10}$$

Hence the total exergy in the TES at any time ‘t’ can be written as,

$$\xi_t = \sum_{i=1}^{n} \rho_i V_i C_{P_i} \left[(T_{i.t} - T_0) + T_0 \ln\left(\frac{T_0}{T_{i,t}}\right)\right] \tag{11}$$

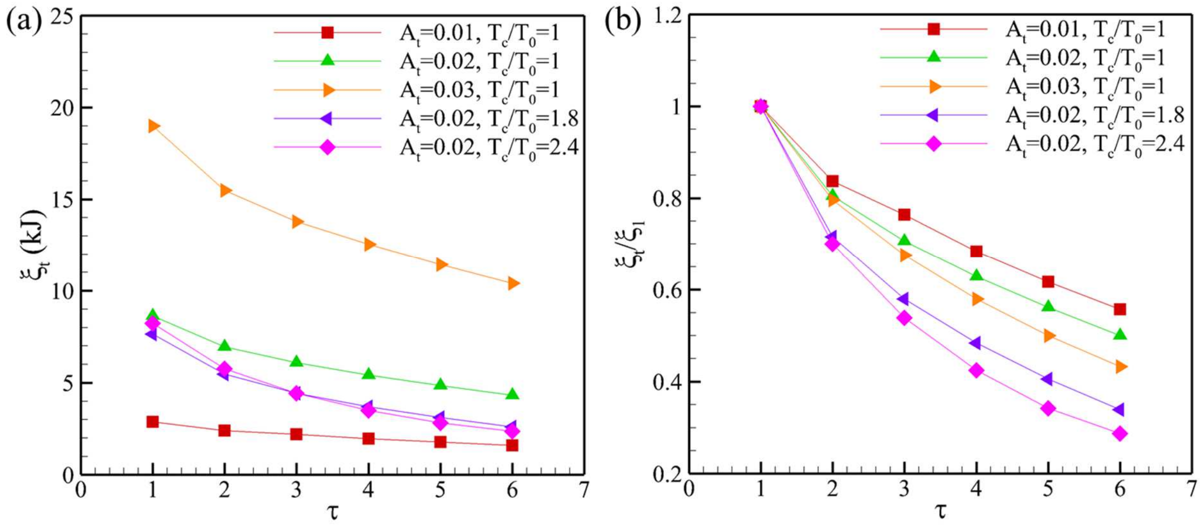

Figure 8 (Colour): (a) The exergy ξ_t in TES is plotted against normalised storage time instant $\tau = t/t_1$ (b) The normalised exergy $\xi^{\#} = \xi_t/\xi_1$ is plotted against normalised storage time instant $\tau = t/t_1$

A comparison of exergy (available energy) magnitude (Figure 8) indicates that, in the case of the ambient cold fluid condition, higher the Atwood number, higher is the magnitude of available energy. Upon doubling T_h (i.e., $A_t = 0.01$ to $A_t = 0.03$), the exergy is found to increase by 5.65 times, at the initial storage instant. Even after 5 hours, the exergy value of A_t= 0.03 is 5.2 times compared to A_t=0.01. However, the rate of exergy decrement is also found to be greater for higher Atwood number case. There is a 12.5% enhancement in the degradation rate observed after 5 hours, when comparing the A_t = 0.01 and 0.03 cases. Thus, relative decay rate of exergy is an increasing function of the Atwood number, as in the case of stored energy.

On the other hand, cases at similar Atwood numbers show the same amount of exergy in the post charging phase. However, a greater rate of decrement of energy is exhibited at higher mean temperature. The extra percentage of exergy decrement of $T_c/T_0 = 2.4$ after 5 hours, in comparison with $T_c/T_0 = 1$ is observed to be 19.5. Thus, for same A_t cases, nearer the mean temperature is to the ambient temperature, the better is the quality of energy stored.

Figure 9 shows the variation of entropy generation rate, for various Atwood number and mean temperature cases. The entropy generation rate is observed to decrease over time and attain a steady value for all the cases. From the graph it is obvious that the entropy generation rate is greater for higher Atwood number cases with same T_c, at all the time instances. One can also observe that upon maintaining same Atwood number, entropy generation rate increases as T_c is increased. Nonetheless, the most interesting observation can be made with cases C, D and E. Cases D and E show higher rate of entropy generation, owing to its higher cold fluid temperature T_c as compared to case C.

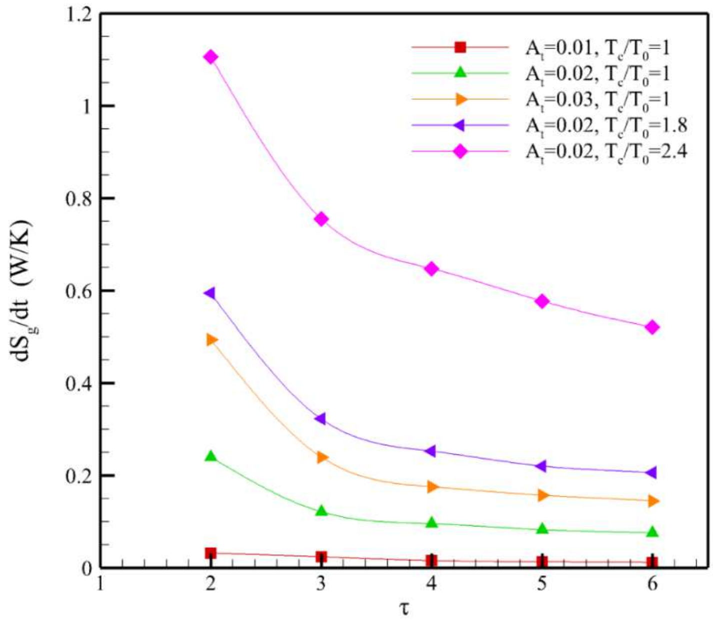

Figure 9 (Colour): (a) The exergy ξ_t in TES is plotted against normalised storage time instant $\tau = t/t_1$ (b) The normalised exergy $\xi^{\#} = \xi_t/\xi_1$ is plotted against normalised storage time instant $\tau = t/t_1$

It can be concluded from this experimental study that better utilitzation of the TES with higher potential for energy storage is possible if the temperature difference between the two fluids is higher and the cold fluid temperature is near the ambient condition. Although the rate of decrement is higher, this is the most effective way of storing the maximum energy without losing much quality in case of a stratified TES.

3.4. Comparison with fully mixed TES

For each scenario, the ratio of the exergy of the stratified storage at any time t, (ξ_t) to that of the same storage when fully mixed (ξ_m) is estimated as per Dincer et.al [21] (Figure 10). ξ_m is obtained from the following formula:

$$\xi_m = E_m - mc_pT_0 \ln(T_m/T_0) \qquad (12)$$

Where, $T_m = \frac{1}{n}\sum_{i=1}^{n} T_{i,t}$ represents the temperature of the TES fluid at the fully mixed state and

$$E_m = mc_p(T_m - T_0) \qquad (13)$$

is the energy of a fully mixed tank at that uniform temperature T_m

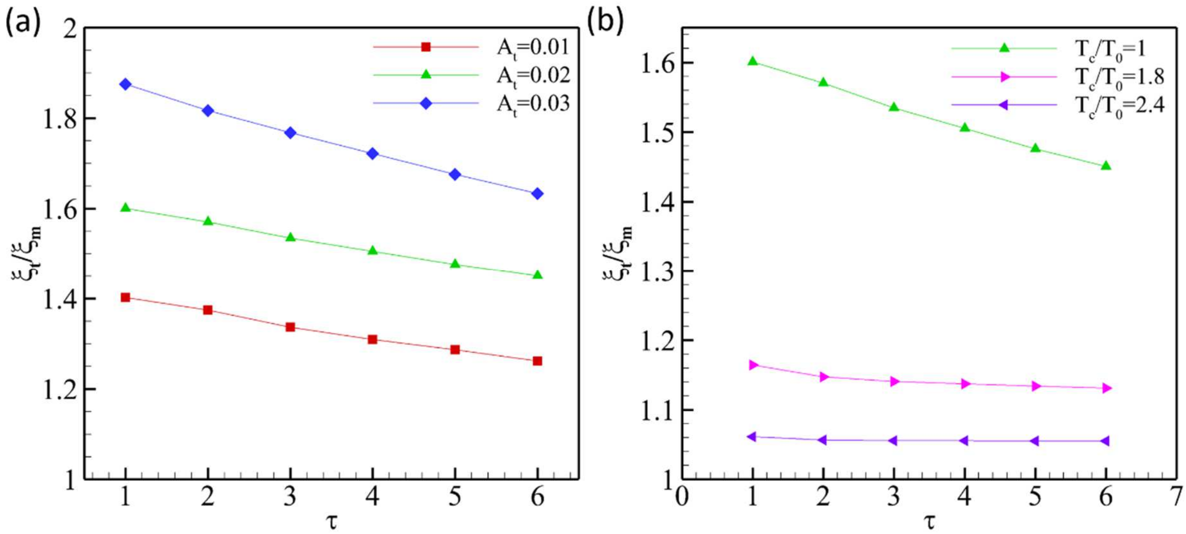

Figure 10 (Colour): The normalised exergy $\xi^* = \xi_t/\xi_m$ as per Dincer et.al [21] is plotted against normalised storage time instant $\tau = t/t_1$ for cases (a) With ambient cold fluid condition, $T_c/T_0 = 1$ but distinct Atwood numbers (b) With same $\Delta T = (T_h - T_c) = 50^0 C$ and approximately same A_t=0.02 but distinct cold fluid temperature T_c

Figure 10 shows the extra energy stored by the stratified TES as compared to the mixed case. For example, ξ_t/ξ_m =1.4 indicates that the exergy of the stratified storage is about 40% greater than the exergy of the mixed storage. Therefore, stratification increases the exergy storage capacity of the storage under consideration, relative to its mixed condition. Figure 10 also depicts that it is advantageous to increase A_t by keeping T_c/T_0 constant (Figure 10a), and keeping the cold fluid temperature near ambient conditions (Figure 10b).

4. Conclusion

The present work is an experimental investigation on establishing a stable single medium thermocline-based TES within a single tank for a suitably long time. The study sheds light on not only the design and development of SMT but also an experimental procedure to establish such storage. The experimental results are analyzed using the first and second laws of thermodynamics. We also presented how the effectiveness of the thermal energy storage varies. The results show the impact of the mean temperature and Atwood number on storage effectiveness. We have experimentally shown that by increasing A_t, one could minimize such risks and form a more effective stratification which could sustain for longer durations. However, one should provide sufficient internal insulation to TES to mitigate potential heat loss via axial conduction through TES wall.

Experimental observations indicate that, upon doubling T_h from 50^0C to 100^0C by keeping T_c constant, the exergy is found to increase by 5.65 times, at the initial storage instant. Upon keeping A_t constant, the percentage exergy decrement of $T_c/T_0 = 2.4$ after 5 hours is observed to be 19.5% more than that of $T_c/T_0 = 1$. Thus, for the same initial temperature difference between the fluids (ΔT), the cases with mean temperature greater than the ambient, show higher thermal energy and exergy efficiency but at the cost of greater degradation rate. In case of similar Atwood number, near-ambient mean temperature has better utility. In short, higher Atwood number (stratification) with near ambient - T_c favours TES usefulness. This makes the very commonly used heat storage material molten-salt, a less preferred one for

SMT based TES. Although molten salt has a higher operating range, it is in solid phase at room temperature and requires significantly high temperature for melting. Hence one requires to maintain a significantly higher Atwood number for its best utilisation. Thus, the best suited HSM is a room-temperature liquid with high C_P and high operating range.

Through the study, we could establish a stable and sustainable thermocline for more than 6 hours keeping the fluid dynamic perturbations under control. The facility could be a test bench/certification bed for different thermal storage schemes involving various thermal storage media.

5. Acknowledgement

This paper is based upon work supported in part by the India–US partnership to Advance Clean Energy-Research (PACE-R) for the Solar Energy Research Institute for India and the United States (SERIIUS), funded jointly by the U.S. Department of Energy (Office of Science, Office of Basic Energy Sciences, and Energy Efficiency and Renewable Energy, Solar Energy Technology Program, under Subcontract DE-AC36-08GO28308 to the National Renewable Energy Laboratory, Golden, Colorado) and the Government of India, through the Department of Science and Technology under Subcontract IUSSTF/JCERDC-SERIIUS/2012 dated 22nd November 2012.

6. References

[1]. United Nations, "Transforming our world : the 2030 Agenda for Sustainable Development," 2015.
[2]. H. L. Zhang, J. Baeyens, J. Degrève, and G. Cacères, "Concentrated solar power plants: Review and design methodology," Renew. Sustain. energy Rev., vol. 22, pp. 466–481, 2013.
[3]. I. Sarbu and C. Sebarchievici, "A comprehensive review of thermal energy storage," Sustainability, vol. 10, no. 1, p. 191, 2018.
[4]. K. E. Elfeky, X. Li, N. Ahmed, L. Lu, and Q. Wang, "Optimization of thermal performance in thermocline tank thermal energy storage system with the multilayered PCM(s) for CSP tower plants," Appl. Energy, vol. 243, pp. 175–190, Jun. 2019, doi: 10.1016/J.APENERGY.2019.03.182.
[5]. L. F. C. Andrea Frazzica, Recent Advancements in Materials and Systems for Thermal Energy Storage. 2019.
[6]. A. Gil et al., "State of the art on high temperature thermal energy storage for power generation. Part 1—Concepts, materials and modellization," Renew. Sustain. Energy Rev., vol. 14, no. 1, pp. 31–55, 2010.
[7]. Z. Lavan and J. Thompson, "Experimental study of thermally stratified hot water storage tanks," Sol. Energy, vol. 19, no. 5, pp. 519–524, Jan. 1977, doi: 10.1016/0038-092X(77)90108-6.
[8]. B. J. Sliwinski, A. R. Mech, and T. S. Shih, "Stratification in thermal storage during charging," in 6th International Heat Transfer Conference, Toronto, ON, Canada, Aug, 1978, pp. 7–11.
[9]. R. I. Loehrke, J. C. Holzer, H. N. Gari, and M. K. Sharp, "Stratification Enhancement in Liquid Thermal Storage Tanks," J. Energy, vol. 3, no. 3, pp. 129–130, May 1979, doi: 10.2514/3.62425.

[10]. H. Price, "Parabolic trough solar power plant simulation model," 2003.
[11]. S. M. Flueckiger, B. D. Iverson, S. V. Garimella, and J. E. Pacheco, "System-level simulation of a solar power tower plant with thermocline thermal energy storage," Appl. Energy, vol. 113, pp. 86–96, Jan. 2014, doi: 10.1016/j.apenergy.2013.07.004.
[12]. F. G. F. Qin et al., "Thermocline stability criterions in single-tanks of molten salt thermal energy storage," Appl. Energy, vol. 97, pp. 816–821, Sep. 2012, doi: 10.1016/j.apenergy.2012.02.048.
[13]. M. Y. Haller, W. Streicher, E. Andersen, and S. Furbo, "Compararative analysis of thermal energy storage stratification efficiency – a new method combines advantages," no. 2008, 2009.
[14]. Y. M. Han, R. Z. Wang, and Y. J. Dai, "Thermal stratification within the water tank," Renew. Sustain. Energy Rev., vol. 13, no. 5, pp. 1014–1026, Jun. 2009, doi: 10.1016/J.RSER.2008.03.001.
[15]. J. E. Pacheco, S. K. Showalter, and W. J. Kolb, "Development of a Molten-Salt Thermocline Thermal Storage System for Parabolic Trough Plants," J. Sol. Energy Eng., vol. 124, no. 2, p. 153, 2002, doi: 10.1115/1.1464123.
[16]. T. Esence, A. Bruch, S. Molina, B. Stutz, and J.-F. Fourmigué, "A review on experience feedback and numerical modeling of packed-bed thermal energy storage systems," Sol. Energy, vol. 153, pp. 628–654, 2017.
[17]. G. Zanganeh, A. Pedretti, S. Zavattoni, M. Barbato, and A. Steinfeld, "Packed-bed thermal storage for concentrated solar power--Pilot-scale demonstration and industrial-scale design," Sol. Energy, vol. 86, no. 10, pp. 3084–3098, 2012.
[18]. A. Bruch, S. Molina, T. Esence, J. F. Fourmigué, and R. Couturier, "Experimental investigation of cycling behaviour of pilot-scale thermal oil packed-bed thermal storage system," Renew. energy, vol. 103, pp. 277–285, 2017.
[19]. S. M. Flueckiger, Z. Yang, and S. V Garimella, "Thermomechanical simulation of the solar one thermocline storage tank," J. Sol. energy Eng., vol. 134, no. 4, 2012.
[20]. S. Molina, D. Haillot, A. Deydier, and J. P. Bedecarrats, "Material screening and compatibility for thermocline storage systems using thermal oil," Appl. Therm. Eng., vol. 146, no. March 2018, pp. 252–259, 2019, doi: 10.1016/j.applthermaleng.2018.09.094.
[21]. I. Dincer, "On thermal energy storage systems and applications in buildings," Energy Build., vol. 34, no. 4, pp. 377–388, 2002.
[22]. C. Mira-Hernández, S. M. Flueckiger, and S. V. Garimella, "Numerical simulation of single- and dual-media thermocline tanks for energy storage in concentrating solar power plants," Energy Procedia, vol. 49, pp. 916–926, 2014, doi: 10.1016/j.egypro.2014.03.099.
[23]. C. Mira-Hernández, S. M. Flueckiger, and S. V Garimella, "Comparative analysis of single- and dual-media thermocline tanks for thermal energy storage in concentrating solar power plants," J. Sol. Energy Eng., vol. 137, no. 3, 2015.
[24]. P. Gajbhiye, N. Salunkhe, S. Kedare, and M. Bose, "Experimental investigation of single media thermocline storage with eccentrically mounted vertical porous flow distributor," Sol. Energy, vol. 162, no. September 2017, pp. 28–35, 2018, doi: 10.1016/j.solener.2017.12.062.
[25]. S. Advaith, K. V Manu, A. Tinaikar, U. K. Chetia, and S. Basu, "Interaction of vortex ring with a stratified finite thickness interface," Phys. Fluids, vol. 29, no. 9, p. 93602, 2017.
[26]. K. V. Manu, P. Anand, U. K. Chetia, and S. Basu, "Effects of instabilities and coherent structures on the performance of a thermocline based thermal energy storage," Appl. Therm. Eng., vol. 87, pp. 768–778, Aug. 2015, doi: 10.1016/j.applthermaleng.2015.05.072.

Appendix A

Table 2: Component details and specifications of the laboratory scale facility

Component	Specifications	Make
Pump	Vertical, Non- Clog Type, Water cooled Centrifugal, Mitsubishi VFD (FR-D720) controlled, Head: 30m, Impeller type: Semi Open, Motor: 7.5HP, RPM: 2900, Temperature: 800^{0}C with external cooling	Process Pumps(I) Pvt. Ltd
Pneumatic Control Valves	Diaphragm Type Single Acting Actuator, Working Pressure 2.5 to 3.5 Kg/cm^2 Model-PKH, Globe Type 2/2 Way – 3/2 Way, 1″, Body-S.S.304, Pressure- up to 10 Bar, Temperature up to 450°C	Aira Euro Automation Pvt. Ltd.
Piping	1' NB, Sch- 40, Inconel-600	Process Pumps(I) Pvt. Ltd
Flow distributor	Diameter: 150 mm, thickness- 15mm. approx. no. of holes: 132, Hole diameter: 5 mm	Process Pumps(I) Pvt. Ltd
Flow measuring device	Promass F High temperature version, Coriolis multi-purpose, DN 50, Range: 0-18000 Kg/h, Maximum measured error: Mass flow: ±0.05% of reading, Density: ±0.01 g/cc	Endress Hauser Pvt. Ltd
Split-type cartridge heater	Heat rating: 10×2.5 kW, inbuilt cooling system with exhaust, MOC: SS304, Length: 800mm, Operating temperature (max.): 750^{0}C, Flux density (max.):18 W/cm^2 (with flow)	Heatcon Pvt. Ltd
Flanged immersion heater	Heat rating: 3×3.3 kW, MOC: SS304, Length: 450mm, Operating temperature (max.): 650^{0}C, Flux density (max.):15.5 W/cm^2	Heatcon Pvt. Ltd
Thermocouples	K type (Chromel - Alumel), total numbers: 150, Accuracy: $\mp$0.75K	Heatcon Pvt. Ltd
Data logging system	PID controllers (RS-485), Compact DAQ system, connected to the PC through USB and operated with NI-DAQmx driver software	Heatcon Pvt. Ltd, National Instruments